

## Cordierite II: The role of CO<sub>2</sub> and H<sub>2</sub>O

B.A. KOLESOV<sup>1</sup> AND C.A. GEIGER<sup>2,\*</sup>

<sup>1</sup>Institute of Inorganic Chemistry, Lavrentiev prosp. 3, Novosibirsk 630090, Russia

<sup>2</sup>Institut für Geowissenschaften, Universität Kiel, Olshausenstrasse 40, 24098 Kiel, Germany

### ABSTRACT

Polarized single-crystal Raman spectra at room temperature and 5 K and polarized infrared spectra at room temperature were obtained from four natural cordierites of different compositions in the wave number region of the CO<sub>2</sub> symmetric stretching vibration and the H<sub>2</sub>O stretching vibrations. The CO<sub>2</sub> molecules are preferentially aligned parallel to the X axis, consistent with results from X-ray diffraction and optical studies. The CO<sub>2</sub> contents of six natural cordierites, previously studied by powder IR methods (Vry et al. 1990), were determined via Raman spectroscopy. A linear relationship was found between CO<sub>2</sub> content and the Raman intensity ratio of the normalized CO<sub>2</sub> stretching mode against a Si-O stretching mode. This permits a determination of the CO<sub>2</sub> contents in cordierite using micro-Raman measurements. The internal stretching modes between 3500 and 3800 cm<sup>-1</sup> were assigned to various types of H<sub>2</sub>O molecules occurring in the channel cavity. Three different orientations of H<sub>2</sub>O molecules that have no interactions with alkali cations located at 0,0,0 in the six-membered tetrahedral rings are classified in a static model as Class I H<sub>2</sub>O molecules. The H-H vector for two of them is parallel to [001], and their molecular planes lie in the XZ and YZ crystal planes. The third type has its H-H vector directed along the X axis and its molecular plane lies in the XZ plane. Two other types of H<sub>2</sub>O have interactions with the alkali cations located at 0,0,0. They are classified as Class II H<sub>2</sub>O. They distinguish themselves by the number of H<sub>2</sub>O molecules bonded to the alkali atoms. The formation of weak hydrogen bonds at low temperatures may explain the appearance of some Raman stretching modes below 200 K. The H<sub>2</sub>O molecules of Class I-Type I/II are probably dynamically disordered about [001] hopping between orientations in the XY and XZ planes down to 5 K. Class II H<sub>2</sub>O may also be disordered, but more measurements are required to describe its dynamic behavior.

### INTRODUCTION

The incorporation and orientation of molecular CO<sub>2</sub> and H<sub>2</sub>O in the channel cavities of cordierite, (Mg,Fe)<sub>2</sub>Al<sub>4</sub>Si<sub>5</sub>O<sub>18</sub>X(H<sub>2</sub>O, CO<sub>2</sub>) were investigated using various experimental and computational methods including DTA and dehydration studies (Sugiura 1959), X-ray and neutron diffraction (e.g., Cohen et al. 1977; Armbruster 1985), IR spectroscopy (Farrell and Newnham 1967; Goldman et al. 1977; Vry et al. 1990), proton NMR spectroscopy (Carson et al. 1982), quasi-elastic neutron scattering (Winkler et al. 1994b), and quantum mechanical calculations (Winkler et al. 1994a). These various studies show that CO<sub>2</sub> is aligned parallel to the X axis of cordierite (Armbruster and Bloss 1982; Armbruster and Bürgi 1982; Aines and Rossman 1984; Armbruster 1985). The behavior of H<sub>2</sub>O is more complicated. Farrell and Newnham (1967) found that the H<sub>2</sub>O molecules lie in the XZ crystal plane (010) with the H-H direction parallel to the channel axis [001]. Goldman et al. (1977), following upon the work of Wood and Nassau (1967) in beryl, concluded that two types of H<sub>2</sub>O molecules can be identified, which they labeled as Type I and II. The molecular plane of both Type I and II H<sub>2</sub>O is located in the YZ crystal

plane (100), but they differ in the orientation of their H-H vectors, which are either parallel (Type I) or perpendicular (Type II) to [001]. The apparent discrepancy over the orientation of the H<sub>2</sub>O molecular plane proposed by Farrell and Newnham (1967) vs. Goldman et al. (1977) can be explained by the different crystal settings used by the two groups. From neutron diffraction results, Cohen et al. (1977) proposed that the H<sub>2</sub>O molecules are statistically disordered over four different orientations with their molecular plane nearly parallel to the XY crystal plane (001). Hochella et al. (1979) proposed, using X-ray methods and a reinterpretation of the neutron diffraction data, that the molecular plane of H<sub>2</sub>O is tilted about 29° from (100). Winkler et al. (1994b) proposed that Type I H<sub>2</sub>O in synthetic Mg-cordierite is rotationally disordered about [001] and that a pure static description is inappropriate to describe its behavior in the channel cavity. They proposed a two orientation jump model in which the H-H vector remains parallel to [001] and the H<sub>2</sub>O molecule rotates about its center of mass with an estimated jump time of about 6 ps at room temperature. There is no information on the dynamics of Type II H<sub>2</sub>O.

Infrared spectroscopy is a powerful method for the detection and description of H<sub>2</sub>O. However, unexplained inconsistencies or problems exist regarding the band assignments for Type I H<sub>2</sub>O. In the case of cordierite it was shown that the interaction between H<sub>2</sub>O and the silicate framework is very weak (Langer and Schreyer 1976; Winkler et al. 1994a).

\*E-mail: nmp46@rz.uni-kiel.de

Goldman et al. (1977) reported  $\nu_1$  and  $\nu_3$  mode energies for Type I H<sub>2</sub>O at ~3650 and 3689 cm<sup>-1</sup>, respectively. However, the wave numbers of  $\nu_1$  and  $\nu_3$  of free H<sub>2</sub>O in solid inert matrixes are well known. They occur at 3634.5 and 3726.9 cm<sup>-1</sup> in solid nitrogen (Nelander 1985; Fredin et al. 1977), 3619 and 3733 cm<sup>-1</sup> in solid argon (Redington and Milligan 1962), and 3633.6 and 3731.7 cm<sup>-1</sup> in solid oxygen (Tso and Lee 1984). The difference in wave numbers between the two is about 100 cm<sup>-1</sup>. First principle calculations on the H<sub>2</sub>O molecule also give a difference of about 100 cm<sup>-1</sup>. Thus, it is unclear why the proposed difference between  $\nu_1$  and  $\nu_3$  of Type I H<sub>2</sub>O in cordierite (~40 cm<sup>-1</sup>) is so small. The wave number difference,  $\Delta\nu$ , between  $\nu_3$  and  $\nu_1$  of Type II H<sub>2</sub>O is 58 cm<sup>-1</sup>, which is also small. Here, however, the H<sub>2</sub>O interacts with an alkali metal (K, Na) located at 0,0,0 in the center of six-membered rings and, therefore, need not have  $\Delta\nu$  of a free H<sub>2</sub>O molecule. In addition to this discrepancy, the IR spectra presented by Farrell and Newnham (1967) and Goldman et al. (1977) contain two additional modes at ~3710 and ~3600 cm<sup>-1</sup> that were not considered in their spectral analysis and band assignments. It is not clear what they represent.

Here we investigate the CO<sub>2</sub> and H<sub>2</sub>O molecules in natural cordierites of different Fe<sup>2+</sup>/(Mg + Fe<sup>2+</sup>) ratios and in a sample with substantial channel alkali cations using polarized single-crystal Raman spectroscopy and polarized IR spectroscopy. Raman and IR spectroscopy, together, give a nearly complete picture of the vibrational behavior (polarizability tensor and dipole momentum) of CO<sub>2</sub> and H<sub>2</sub>O in the cavities of cordierite. For the case of CO<sub>2</sub>, the polarization direction of the asymmetric  $\nu_3$  mode in the IR or symmetric  $\nu_1$  mode in the Raman gives the orientation of the CO<sub>2</sub> molecular axis. A determination of the orientation of the H<sub>2</sub>O molecule and an assignment of the different internal vibrations is straightforward when both types of spectroscopic data are used and when information on the known energies of vibration of a free H<sub>2</sub>O molecule are considered. In both the Raman and IR all internal H<sub>2</sub>O vibrations are active. In the IR the polarization of the asymmetric stretch,  $\nu_3$ , gives the direction of the H-H vector directly, while the polarization of the symmetric stretch,  $\nu_1$ , gives the orientation of the molecular plane. However, this is difficult in practice, because  $\nu_1$  is not strong in the IR. Thus additional information from the Raman active modes is needed. Here  $\nu_3$  is weak, but  $\nu_1$  is stronger. In Raman spectroscopy one should know independently the  $\alpha_{xx}$ ,  $\alpha_{yy}$ , and  $\alpha_{zz}$  polarizabilities along the H<sub>2</sub>O axes of the molecule. Then the intensity of the  $\nu_1$  mode can be measured for the various crystallographic directions in cordierite and the orientation of H<sub>2</sub>O in the channel cavities determined.

A description and an understanding of the role of both molecules in cordierite pertains to the energetics and structural interactions between guest molecules and porous host phases of a variety of structures. Such information is needed in petrologic investigations of the composition of the fluid phase present during metamorphism (e.g., Vry et al. 1990). Laboratory determinations of the H<sub>2</sub>O and CO<sub>2</sub> contents of synthetic Mg-cordierite as a function of  $P$  and  $T$  (e.g., Johannes and Schreyer 1981; Le Breton and Schreyer 1993) have met with mixed success. Raman spectroscopy offers the possibility to better character-

ize H<sub>2</sub>O and CO<sub>2</sub> in cordierite, because it can be used to determine both their amounts and orientation and at a high spatial resolution with relatively little sample preparation. However, only through a combined use of different spectroscopic methods can a complete description of H<sub>2</sub>O in cordierite be made.

## EXPERIMENTAL METHODS

Four cordierite samples were chosen for detailed study and six more for the determination of their CO<sub>2</sub> contents. The detailed study includes two Mg-rich samples—one from Madagascar and one nearly end-member Mg-cordierite probably from Sri Lanka. (The samples are from the study of Shannon et al. 1992 and have the labels 56163-90 and 56163-92, respectively, G.R. Rossman, personal communication.) The third sample is an Fe-rich cordierite from Dolni Bory in the Czech Republic (TUB-1 from the TU-Berlin collection) and the fourth an alkali-rich cordierite from Haddam, Connecticut, U.S.A. (an X-ray single-crystal refinement of this Haddam cordierite is given in Armbruster 1986). Compositions as determined by electron microprobe are in Table 1. The six samples used here just for CO<sub>2</sub> determination using Raman methods are the same cordierites used in an IR investigation by Vry et al. (1990) and are described in their Table 1 (Nos. 3, 10, 12, 25, 27, and 32). All samples are low cordierite, space group *Cccm* with  $a = 17.7$ ,  $b = 9.7$ , and  $c = 9.3$  Å.

Polarized single-crystal Raman spectra were recorded with a Triplemate, SPEX spectrometer with a CCD detector, model LN-1340PB, from Princeton Instruments. The 488 nm and 514 nm lines of an Ar-laser were used for excitation. The spectra at

TABLE 1. Chemical composition of cordierites

| Sample Location                          | TUB-1 Dolni Bory† | TA-1 Haddam‡ | RS-1* Madagascar§ | RS-2* Sri Lankall |
|--|-------------------|--------------|-------------------|-------------------|
| <b>Oxide wt%</b>                         |                   |              |                   |                   |
| SiO <sub>2</sub>                         | 45.34             | 48.13        | 49.48             | 50.61             |
| TiO <sub>2</sub>                         | 0.02              | 0.01         | 0.00              | 0.01              |
| Al <sub>2</sub> O <sub>3</sub>           | 32.11             | 31.14        | 33.52             | 34.15             |
| MgO                                      | 2.23              | 8.69         | 11.43             | 13.38             |
| FeO                                      | 16.89             | 6.51         | 3.73              | 0.83              |
| MnO                                      | 0.79              | 0.39         | 0.16              | 0.01              |
| CaO                                      | 0.05              | 0.01         | 0.00              | 0.00              |
| K <sub>2</sub> O                         | 0.00              | 0.01         | 0.02              | 0.00              |
| Na <sub>2</sub> O                        | 0.56              | 1.49         | 0.20              | 0.17              |
| Total                                    | 97.99             | 96.38        | 98.54             | 99.16             |
| <b>Cations</b>                           |                   |              |                   |                   |
| Si                                       | 4.91              | 5.05         | 4.98              | 4.99              |
| Al                                       | 4.10              | 3.85         | 3.98              | 3.97              |
| Σ (tet.)                                 | 9.01              | 8.90         | 8.96              | 8.96              |
| Mg                                       | 0.36              | 1.84         | 1.72              | 1.97              |
| Fe <sup>2+</sup>                         | 1.53              | 0.22         | 0.31              | 0.07              |
| Mn <sup>2+</sup>                         | 0.07              | 0.04         | 0.01              | 0.00              |
| Σ (oct.)                                 | 1.96              | 2.10         | 2.04              | 2.04              |
| Na                                       | 0.12              | 0.30         | 0.04              | 0.03              |
| K  | 0.00              | 0.00         | 0.00              | 0.00              |
| Σ (channel)                              | 0.12              | 0.30         | 0.04              | 0.03              |
| <b>Fe<sup>2+</sup> mole fraction</b>     |                   |              |                   |                   |
| Fe <sup>2+</sup> /(Fe <sup>2+</sup> +Mg) | 0.84              | 0.12         | 0.16              | 0.03              |

Note: Calculated on the basis of 18 oxygens per anhydrous formula unit.

\* Analyses from Shannon et al. (1992).

† Granitic pegmatite.

‡ Pegmatite.

§ Metamorphic.

ll Location uncertain, probably metamorphic.

room temperature were obtained in back-scattering geometry using a conventional micro Raman setup. The laser beam was focused to a diameter of 2 micrometers using a LD-EPIPLAN, 40/0.60 pol., Zeiss objective with a numerical aperture of 0.6. The spectral slit was 5 cm<sup>-1</sup>. The spectra at low temperatures were obtained in a 90° scattering geometry, where the crystal was fixed onto a cold finger of a helium cryostat (APD Cryogenic Inc., model LT-3-110). The low-temperature experiments were made with a spectral slit of 2 cm<sup>-1</sup>. The spectra are characterized by a simplified Porto's notation, where the first symbol gives the polarization direction of the incident light and the second one the polarization direction of the scattered light.

The polarized single-crystal infrared measurements were made on the Sri Lanka cordierite at room temperature. A Bruker IFS 66V/S spectrometer with a microscope attachment was used. Thin orientated crystal platelets of 25 μm thickness were prepared, because of the strong absorption given by the H<sub>2</sub>O stretching vibrations. Measurements were made along the directions of the three crystal axes with 512 scans at a spectral resolution of 2 cm<sup>-1</sup>.

## RESULTS AND DISCUSSION

### The orientation and concentration of CO<sub>2</sub> in cordierite

The intensity of the CO<sub>2</sub> stretching mode at 1383 cm<sup>-1</sup> as a function of crystal orientation (Fig. 1) shows that the CO<sub>2</sub> in the channel cavities is preferentially aligned parallel to the X

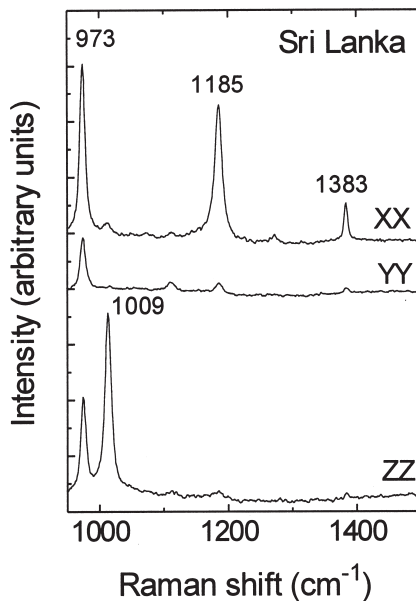


**FIGURE 1.** Polarized single-crystal Raman spectra of Sri Lanka cordierite at room temperature showing the symmetric CO<sub>2</sub> stretching vibration at 1383 cm<sup>-1</sup>. For a free gaseous CO<sub>2</sub> molecule it occurs at about 1387 cm<sup>-1</sup>. The other bands at lower energies are lattice vibrations from the cordierite framework.

axis. The spectra of the Madagascar sample (not shown) are very similar. (The CO<sub>2</sub> contents of the Dolni Bory and Haddam samples are undetectable spectroscopically.) The observed intensities  $I_{XX}$ ,  $I_{YY}$ , and  $I_{ZZ}$  are about 800, 140, and 50 arbitrary units, respectively. The polarization leakage was calculated from the numerical aperture of the objective and is about 30 arbitrary units for the  $I_{YY}$  and  $I_{ZZ}$  spectra. The band at 1383 cm<sup>-1</sup> is not a pure CO<sub>2</sub> stretching mode, but one of two components of a Fermi-doublet and this may give rise to mode intensity in an "improper" direction. Hence, we normalize the intensities of  $I_{YY}$  to 90 and  $I_{ZZ}$  to 0 arbitrary units. From this analysis, only a small fraction of the CO<sub>2</sub>, less than 10%, may be parallel to the Y axis, but this estimate is at the limit of experimental uncertainty (Fig. 1). This Raman spectroscopic-based interpretation is consistent with the X-ray diffraction and optical results of Armbruster (1985) and the IR spectra of Aines and Rossman (1984). This orientation is energetically favored because the cavity size is longer in the X-axis direction compared to the Y-axis direction (e.g., Hochella et al. 1979). This is important for CO<sub>2</sub> molecules having a long length.

From a knowledge of the CO<sub>2</sub> orientation, it is possible to determine the CO<sub>2</sub> content of other cordierite samples from their spectra and to construct a working curve for a Raman-based determination of CO<sub>2</sub> concentrations. An orientation with a crystallographic plane containing the X-axis must be used because of the orientation of the CO<sub>2</sub> molecule. To avoid the difficulties associated with the measurement of absolute Raman mode intensities, we ratioed the intensity of the CO<sub>2</sub> stretching mode to a lattice vibration mode. Figure 2 shows the angular dependence of the intensity ratio of the CO<sub>2</sub> stretch at 1383 cm<sup>-1</sup> vs. the bands at 973 and 1185 cm<sup>-1</sup> in the XY and XZ crystallographic planes. The two latter bands are also observed in XX Raman spectra (Fig. 1) and can be assigned to SiO<sub>4</sub> stretching modes. Both mode intensity ratios are approximately constant in the angular range between X - 30° and X + 30° and may, therefore, be used for this analytical measurement. For the determination of CO<sub>2</sub> contents, the XX spectra of the Sri Lanka cordierite and the six additional cordierites, whose CO<sub>2</sub> content were previously determined (Vry et al. 1990), were measured (Fig. 3). Figure 4 shows the normalized intensities  $I(1383 \text{ cm}^{-1})/I(973 \text{ cm}^{-1})$  and  $I(1383 \text{ cm}^{-1})/I(1185 \text{ cm}^{-1})$  vs. CO<sub>2</sub> content. A reasonable linear trend is apparent. The scatter, we believe, could be related to uncertainties in the determination of the CO<sub>2</sub> or to local differences in CO<sub>2</sub> contents. Vry et al. (1990) determined the CO<sub>2</sub> concentrations from bulk measurements, while we made measurements at a high spatial resolution on a single small cordierite chip. From the curves we can determine the CO<sub>2</sub> content of the Sri Lanka cordierite, for example, as being rather low with about 0.4 wt%.

### Internal mode assignments and classification of the different H<sub>2</sub>O types

Two types of H<sub>2</sub>O were previously identified and described in the literature. Type I and Type II H<sub>2</sub>O are distinguished by the orientation of their H-H vectors, which are either parallel or perpendicular to [001], respectively. This classification cannot, however, be carried over into this study for reasons that will be described below. Therefore, we present a new classifi-

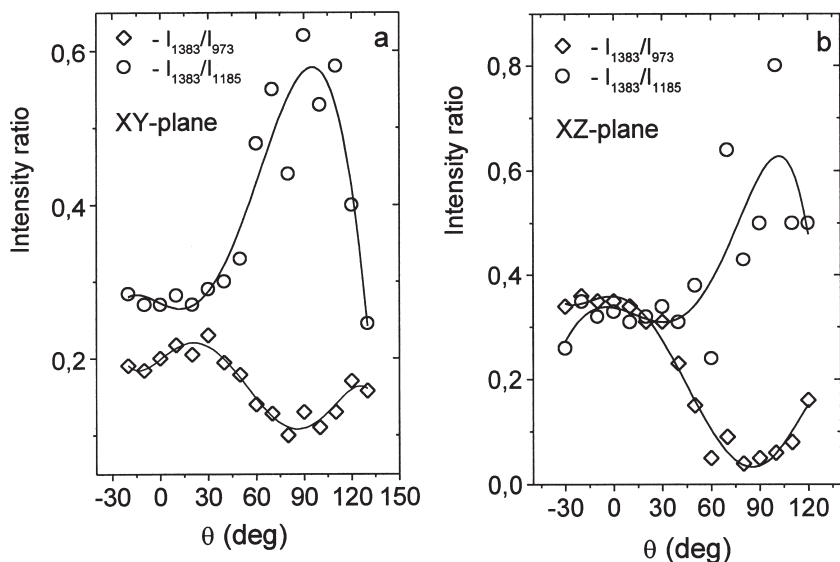


FIGURE 2. The change of the intensity ratio of the CO<sub>2</sub> band at 1383 cm<sup>-1</sup> and the bands at 973 cm<sup>-1</sup> and 1185 cm<sup>-1</sup> (a) in XY and (b) XZ crystallographic planes.

cation scheme, which is constructed as follows: Two Classes, I and II, of H<sub>2</sub>O are described. In the former are placed all types of H<sub>2</sub>O molecules that are located in the channel cavity at about 0,0,1/4 and that are not bonded to or have measurable interactions with cations located at 0,0,0 in the six-membered tetrahedral rings. In the second case, Class II, we place all types of H<sub>2</sub>O molecules which have some kind of interaction with a channel cation. We describe three types of Class I H<sub>2</sub>O and two types of Class II H<sub>2</sub>O in cordierite. Our scheme is based on the following observations and analysis.

The alkali-poor cordierites (Sri Lanka and Madagascar) only show a single  $\nu_1$  Raman mode at 3597 cm<sup>-1</sup>, whereas the alkali-containing-samples (Dolni Bory and Haddam) have two  $\nu_1$  modes at 3597 and 3578 cm<sup>-1</sup> in varying intensity ratios (Fig. 5). The Haddam sample, with more Na, has a more intense band at 3578 cm<sup>-1</sup>. An asymmetric  $\nu_3$  mode at higher wave numbers is not observed at room temperatures. A band at about 3597 cm<sup>-1</sup> is also observed in our polarized IR spectra (Fig. 6) as a weak feature or shoulder in the X, Y, and Z spectra, whereas a stronger  $\nu_1$  band at 3575 cm<sup>-1</sup> is observed in the Z spectrum and appears as a weak shoulder in the X and Y spectra. We assign these two  $\nu_1$  modes to H<sub>2</sub>O molecules belonging to Class I (~3597 cm<sup>-1</sup>) and Class II (~3578 cm<sup>-1</sup>) H<sub>2</sub>O. (Fig. 6 is similar to the spectra in Fig. 7. of Goldman et al. (1977) for a cordierite from Manitouwadge, Canada.) In the IR spectrum with the electric vector parallel to the Z axis (E||Z) three strong bands are present at 3575 and 3683 and 3696 cm<sup>-1</sup>. The latter two are  $\nu_3$  vibrations. In the spectrum with E||Y a broad band at about 3633 cm<sup>-1</sup> is observed and in the E||X spectrum a number of weak bands are seen, but the most important is the strongest at 3708 cm<sup>-1</sup>. At low temperatures, the XZ and YZ Raman spectra resolve bands at 3694 and 3691 cm<sup>-1</sup>, respectively, in the Dolni Bory and Sri Lanka cordierites (Figs. 7 and 8). They are  $\nu_3$  modes having their  $\nu_1$  counterparts at ~3597 cm<sup>-1</sup>, because they lie at wavenumbers about 100 cm<sup>-1</sup> higher. They are extremely weak or not present in the Raman at room temperatures. They define the Class I-Type I and Class I-Type II

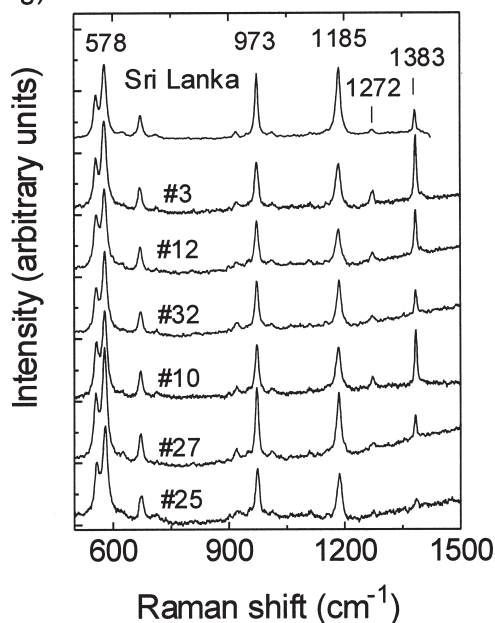


FIGURE 3. Room temperature XX-Raman spectra of the cordierite from Sri Lanka and the six cordierite samples investigated by Vry et al. (1990). The numbers of the samples correspond to those listed in their Table 1.

molecules, respectively. These two different  $\nu_3$  modes are intense and slightly more separated in energy in the IR at room temperature in the Mg-rich Sri Lanka cordierite (Fig. 6), where both occur in the Z spectrum at 3696 and 3683 cm<sup>-1</sup>.

The infrared X spectrum (Fig. 6) shows a moderately strong, sharp band at 3708 cm<sup>-1</sup> that is not observed in any of the Raman spectra. This is a "new"  $\nu_3$  mode not described before, but it is observable in some previously published spectra (see Fig. 7 of Goldman et al. 1977). It is assigned to a new type of H<sub>2</sub>O. It should not be associated with any alkali cation, because it is

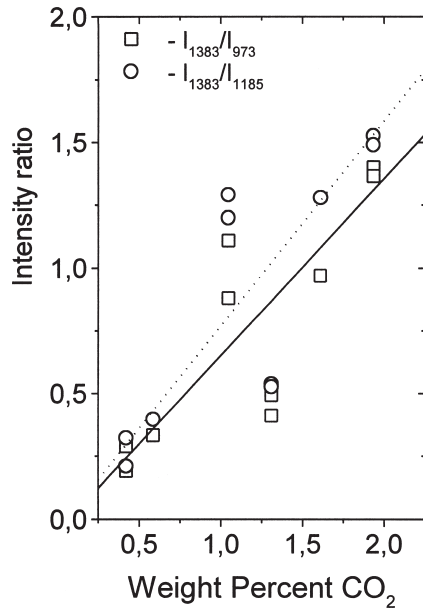


FIGURE 4. The dependence of the  $I_{1383}/I_{973}$  (squares) and  $I_{1383}/I_{1185}$  (circles) band intensity ratios vs. the CO<sub>2</sub> content (as determined by Vry et al. 1990). The solid and dotted lines are linear least-squares best fits to the two data sets.

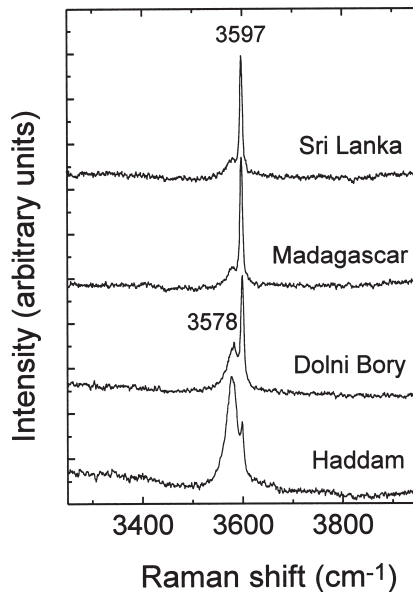


FIGURE 5. Room temperature polarized YY single-crystal Raman spectra showing the symmetric mode,  $\nu_1$ , of the four cordierites of Table 1 in the energy range of the H<sub>2</sub>O stretching vibrations.

found in the Sri Lanka cordierite and because it is located at high wavenumbers. It is assigned to Class I-Type III H<sub>2</sub>O. This band has a narrow FWHH and it could be argued that it is an OH<sup>-</sup> stretching mode. From our data, this possibility can not be ruled out. There could exist crystallographically orientated OH<sup>-</sup> groups in the cordierite framework (Sugiura 1959) or there could be oriented microscopic OH<sup>-</sup> bearing phases in the sample. Its  $\nu_1$  counterpart is difficult to define because it will be very weak, but it should lie around 3595 cm<sup>-1</sup> as in the case of the other two types of Class I H<sub>2</sub>O. This Type III should be most stable in the XZ plane, because the channel cavity is longer along the X direction.

As for Class II H<sub>2</sub>O, two different  $\nu_3$  modes overlap producing a broad band at about 3630 cm<sup>-1</sup> in both the Raman (Figs. 7 and 8) and IR spectra (Fig. 6) at room temperature. In the Raman at 5K, though, the resolution is better and two components at 3626 and 3639 cm<sup>-1</sup> are observed. The intensity of this composite band is related to the amount of alkali cations and is stronger in the Dolni Bory spectrum compared to that of Sri Lanka. They are seen in both XZ and YZ spectra, but their intensity in YZ is approximately five times larger than in XZ. They are present in the IR as an asymmetric broad band at ~3633 cm<sup>-1</sup> in the Y spectrum and a weak broad band at ~3629 cm<sup>-1</sup> in the X spectrum. From this information, we define a Class II-Type I H<sub>2</sub>O as having a  $\nu_3$  mode at 3626 cm<sup>-1</sup> and a Class II-Type II H<sub>2</sub>O as having a  $\nu_3$  mode at 3639 cm<sup>-1</sup> (at 5 K). The two  $\nu_1$  counterparts are difficult to differentiate, but they are around 3571 cm<sup>-1</sup> at 5 K and 3575 cm<sup>-1</sup> at room temperature.

Table 2 classifies the different  $\nu_3$  and  $\nu_1$  H<sub>2</sub>O stretching bands and gives their wave numbers for the IR and Raman spectra at room temperature and 5 K. It also shows the H<sub>2</sub>O orientations

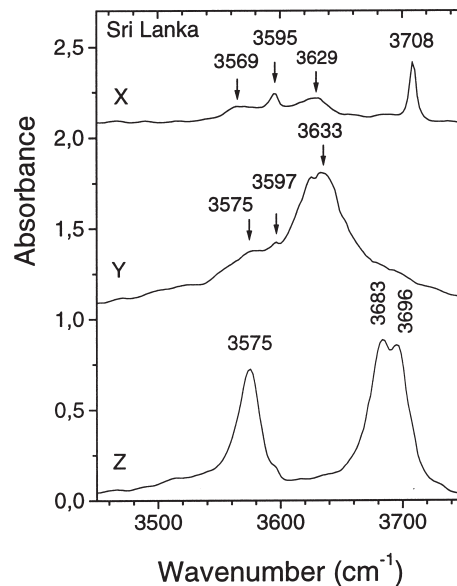


FIGURE 6. Room temperature polarized single-crystal IR absorption spectra of the Sri Lanka cordierite in the energy range of the H<sub>2</sub>O stretching vibrations.

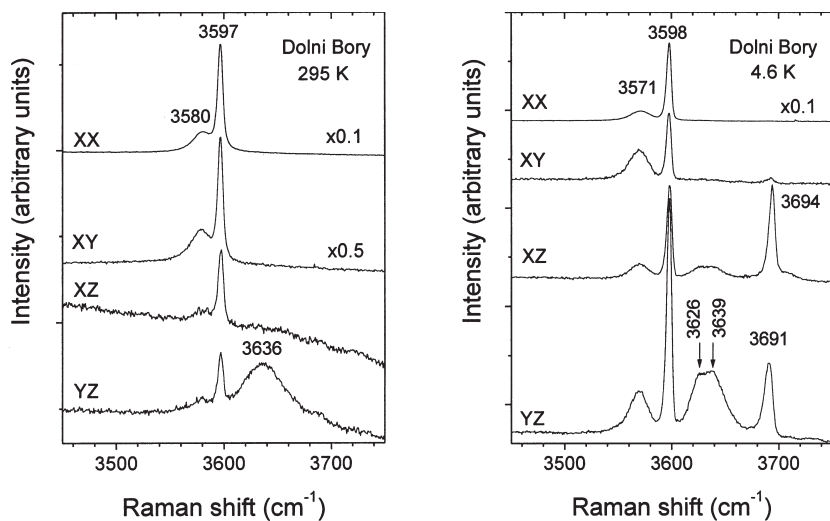


FIGURE 7. Polarized single-crystal Raman spectra of the Dolni Bory cordierite in the energy range of the H<sub>2</sub>O stretching vibrations at room temperature (left) and 5 K (right).

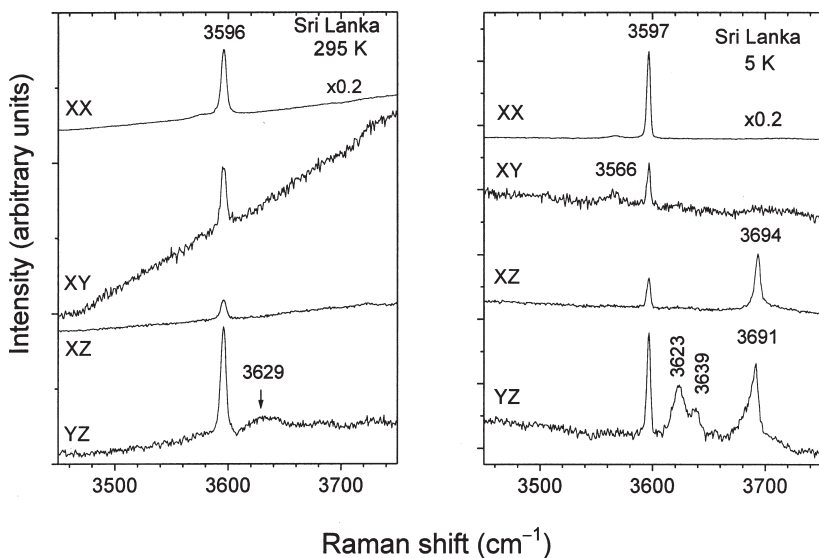


FIGURE 8. Polarized single-crystal Raman spectra of the Sri Lanka cordierite in the energy range of the H<sub>2</sub>O stretching vibrations at room temperature (left) and 5 K (right).

for each type relative to the orthorhombic crystal axes as discussed below.

#### The orientations of Class I—Types I, II, and III H<sub>2</sub>O

In theory, the orientation of H<sub>2</sub>O can be determined unambiguously from its IR spectra, because the polarization of the  $\nu_3$  mode gives the direction of the H—H vector and the polarization of the  $\nu_1$  mode gives the orientation of the molecular plane. However, the problem of determining the H<sub>2</sub>O orientation using IR spectra alone is difficult in practice to solve, because  $\nu_1$  is very weak or not observed for a free molecule, at least not at room temperature. This is true for Class I H<sub>2</sub>O in cordierite and is the same in beryl (Kolesov and Geiger 2000). One needs information from the Raman active modes, in addition, to obtain a complete description of the internal molecular vibrations. In the Raman, the intensity of the  $\nu_1$  mode along the X, Y, and Z axes

defines the H—H direction, while the polarization direction of the  $\nu_3$  mode gives the orientation of the molecular plane. So, for example, the angular dependencies of the Raman intensity of the  $\nu_1$  mode at 3597 cm<sup>-1</sup> at room temperature for the Sri Lanka cordierite (Fig. 9) show that no Class I H<sub>2</sub>O molecules are inclined with respect to any crystallographic axis. Their molecular planes coincide with the those of the crystal. This relationship probably holds for cordierites, but it is not the case in synthetic alkali-free beryl (Kolesov and Geiger 2000).

For Class I Types I and II H<sub>2</sub>O, therefore, their H—H vectors are parallel to the channel axis (i.e., [001]) and the molecules lie in the XZ and YZ crystallographic planes, respectively (Figs. 7 and 8). These two types of H<sub>2</sub>O alone cannot explain, however, the intensity distribution of the  $\nu_1$  mode at 3597 cm<sup>-1</sup> along the X, Y, and Z axes that are 630 ( $I_{XX}$ ), 920 ( $I_{YY}$ ), and 1420 ( $I_{ZZ}$ ) in arbitrary units, respectively (Fig. 9). The first derivatives of

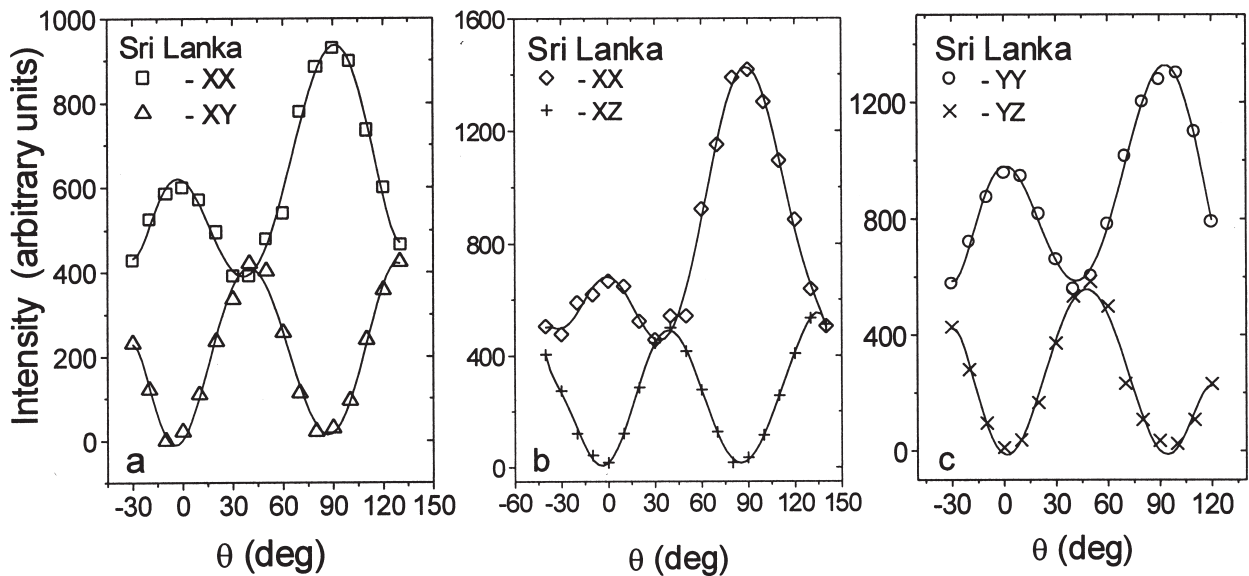


**FIGURE 9.** Angular dependence of the intensity of the  $\nu_1$  Raman mode at  $3597\text{ cm}^{-1}$ . The  $\theta$ -angle is measured (a) from the X to the Y axis, (b) from the X to the Z axis, and (c) from the Y to the Z axis. This shows both parallel and cross polarization of the incident and scattered light relative to the different crystallographic planes. That is, the Raman intensity was measured as the crystal was rotated in about  $10^\circ$  steps in a given crystallographic plane XY or XZ (we use capital letters to denote the crystal axes and small ones the H<sub>2</sub>O molecular axes). These spectra give the intensity of the  $\nu_1$  mode along the three crystallographic axes.

the polarizability,  $\alpha'_{ii}$  ( $i = x, y, z$ ), of  $\nu_1$  for a free H<sub>2</sub>O molecule are 10.3 ( $\alpha'_{xx}$ ), 6.2 ( $\alpha'_{yy}$ ), and 15.1 ( $\alpha'_{zz}$ ) (Murphy 1977 and 1978; Raeymaekers et al. 1988), where the x-molecular axis is parallel to the H-H vector, the y-axis perpendicular to the molecular plane, and the z-axis parallel to the C<sub>2</sub> axis of the molecule. An analysis (where one needs to remember that the Raman intensity is proportional to the square of  $\alpha'_{ii}$ ) shows that there could be at least one additional kind of Class I H<sub>2</sub>O and it should have its H-H vector directed along the X axis and its molecular plane in the XZ plane of the crystal. Indeed, the infrared spectra show a band at  $3708\text{ cm}^{-1}$  in the X spectrum, as well as a very weak  $\nu_1$  shoulder at  $\sim 3595\text{ cm}^{-1}$  in the Z spectrum. These two IR bands can be assigned to this “new” sort of H<sub>2</sub>O, i.e., Class I-Type III H<sub>2</sub>O in cordierite. This is a static description based on the vibrational (Raman and IR) spectra. The possible dynamics will be discussed below.

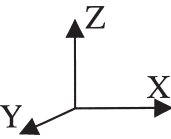
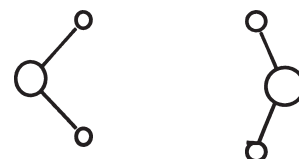
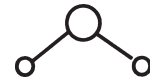
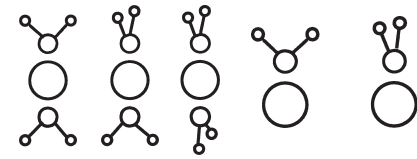
In summary, Class I H<sub>2</sub>O contains three different types of H<sub>2</sub>O in the channel cavity. They are characterized by  $\nu_3$  modes at 3683, 3696, and  $3708\text{ cm}^{-1}$  in Mg-rich alkali-poor cordierite (Table 3) at room temperature and they should have  $\nu_1$  modes around  $3596\text{ cm}^{-1}$ . The exact wave number for the  $\nu_1$  mode of each H<sub>2</sub>O Type is, however, difficult to specify and this is an estimate. The reasons governing the temperature dependence of the Raman stretching modes are more complicated and this question will also be discussed below. First, however, the orientation of the second Class of H<sub>2</sub>O molecules will be discussed.

#### Orientation of Class II—Types I and II H<sub>2</sub>O

Class II H<sub>2</sub>O, by definition, interacts with an alkali metal centered in the six-membered ring at 0,0,0. The unbonded va-

lence-shell electrons of oxygen in H<sub>2</sub>O that determine the bonding properties of a free H<sub>2</sub>O molecule are bonded to the alkali cations in this case. The H-H vector of Class II H<sub>2</sub>O in the alkali-poor Sri Lanka sample is directed along Y (Fig. 6). Its molecular plane lies in the YZ crystal plane and little to no molecules are in the XZ plane (Fig. 8). In the case of the Dolni Bory cordierite the “double”  $\nu_3$  mode is observed in the YZ and XZ Raman spectra and is approximately 5 times more intense in the YZ spectrum (Fig. 7). The two components that are located at  $3626$  and  $3639\text{ cm}^{-1}$  at 5 K maintain the same relative intensities when the polarization direction is changed from YZ to XZ. The two modes are classified as belonging to different Types I and II of H<sub>2</sub>O, because of their different energies. Each type has, however, two possible molecule orientations in the YZ and XZ planes at least for the Dolni Bory sample. We did not observe different energies of the  $\nu_3$  modes for the different molecular orientations. Hence, unlike Class I Type I/II H<sub>2</sub>O, we classify the two sorts only into Types I and II. The FWHH of the  $3639\text{ cm}^{-1}$  mode is about  $20\text{ cm}^{-1}$  and the other at  $3626\text{ cm}^{-1}$  is about  $11\text{ cm}^{-1}$  in the Dolni Bory spectrum as determined by fitting them with Lorentzian peaks. The modes in the Sri Lanka spectrum are similar. We assign the higher energy mode to a configuration Type II, in which superimposing H<sub>2</sub>O molecules in different channel cavities interact with one alkali cation (Table 2). The lower energy band is assigned to a Class II-Type I orientation where just one H<sub>2</sub>O molecule and a neighboring alkali cation interact (Table 2). Kinematic coupling between H<sub>2</sub>O molecules may determine the larger band width of the Type II H<sub>2</sub>O. We state that both types may have at least two different molecular orientations (XZ and YZ planes).

**TABLE 2.** Wavenumber (in cm<sup>-1</sup>), symmetry and assignment of the internal stretching modes of the H<sub>2</sub>O molecules in the static description

|   |         | Class I   |                   |   | Class II   |                                |        |
|---|---------|---|-------------------|---|--|--------------------------------|--------|
|   |         | Type 1  | Type 2            | Type 3  | Type 1   | Type 2                         | Type 2 |
|  |         |  |                   |  |  |                                |        |
| v <sub>1</sub>  | IR*     | ~3595 (RT)  | ~3595 (RT)        | ~3595 (RT)  | 3575 (RT)  | 3575 (RT)                      |        |
|   | Raman * | ~3597 (RT)  | ~3597 (RT)        | ~3597 (RT)  | 3578 (RT)  | 3578 (RT)                      |        |
|   | Raman * | ~3598 (5 K)   | ~3598 (5 K)       | ~3598 (5 K)   | 3571 (5 K)   | 3571 (5 K)                     |        |
| v <sub>3</sub>  | IR      | 3696, Z (RT)  | 3683, Z (RT)      | 3708, X (RT)  | ~3629, X (RT)<br>~3633, Y (RT)   | ~3629, X (RT)<br>~3633, Y (RT) |        |
|   | Raman   | 3696 (Sri Lanka)  | 3691 (Sri Lanka)  |   | 3626 (Dolni Bory)  | 3639 (Dolni Bory)              |        |
|   | Raman   | 3694 (Dolni Bory)   | 3691 (Dolni Bory) |   | XZ, YZ (5 K)   | XZ, YZ (5 K)                   |        |
|   | Raman   | XZ (5 K)  | YZ (5 K)          |   |  |                                |        |

\* These bands are found in all polarization directions of the crystal axes.

### Temperature dependence of the Raman intensity of the v<sub>3</sub> mode

The intensity of the Raman v<sub>3</sub> band(s) of Class I-Type I/II H<sub>2</sub>O changes dramatically as a function of temperature in cordierite. They are not present at room temperature, but are strong at 5 K. Those of Class II H<sub>2</sub>O are observed at both temperatures. These observations are consistent with the different nature of these two Classes of H<sub>2</sub>O molecules and their bonding characteristics. Class II H<sub>2</sub>O interacts with alkali cations in the six-membered rings, while Class I H<sub>2</sub>O is held in place by steric forces at least at room temperature (Wood and Nassau 1968; Winkler et al. 1994a). Hydrogen bonding should be very weak (Langer and Schreyer 1976; Winkler et al. 1994b). The bonding may be different at low temperature. We propose that the reason for the appearance of the v<sub>3</sub> Raman modes at low temperature is due to the formation of weak hydrogen bonds (see also Kolesov and Geiger 2000, for the case in beryl). It is known that the v<sub>3</sub> mode of a free H<sub>2</sub>O molecule is weakly Raman active and the v<sub>1</sub> mode is weak in the infrared. Zilles and Person (1983) have shown that a significant increase in v<sub>1</sub> intensity in the infrared can occur with the formation of a hydrogen bond between two H<sub>2</sub>O molecules. The intensity change is related to charge transfer and dynamical polarization of the hydrogen bond along the direction of it. We propose, therefore, that the Raman v<sub>3</sub> modes of H<sub>2</sub>O molecules of Class I Type I and II appear at lower temperatures due to the formation of hydrogen bonds. Very weak hydrogen bonds may occur between the lone electron pairs of the oxygen atoms of the Si(Al)O<sub>4</sub> tetrahedra of the six-membered rings and H<sub>2</sub>O molecules. Only Class I Types I and II H<sub>2</sub>O have the proper orientation to form hydrogen bonds and, therefore, only they exhibit an increase in their v<sub>3</sub> Raman mode intensities at low temperature. Class I-Type III H<sub>2</sub>O that has its H-H vector aligned parallel to the X axis cannot form hydrogen bonds. Therefore, its v<sub>3</sub> mode is only observed in the infrared (at 3708 cm<sup>-1</sup>) and not in the Raman at any temperature. Class II H<sub>2</sub>O, with its H-H vector perpendicular to [001],

has an orientation which does not allow hydrogen bonds to be formed. This is because the lone electron pairs of the O atoms of the tetrahedra in the center of the cavity wall are directed away from the cavity and cannot bond with the hydrogen atoms. Hence, there is little or no change in their v<sub>3</sub> mode intensity with decreasing temperature.

### Dynamic aspects and analytical determinations of H<sub>2</sub>O in cordierite

Much has been written in the literature about the nature of H<sub>2</sub>O in cordierite. The original IR work assumed at static state for both Classes (formerly types) of H<sub>2</sub>O based on measurements made at room temperature and 77 K (Goldman et al. 1977). At higher temperatures Aines and Rossman (1984) proposed that H<sub>2</sub>O begins to enter a free isotropic unbound state. The inelastic neutron scattering data suggest that Class I-Type I/II H<sub>2</sub>O (Type I in the older notation) is rotationally disordered (Winkler et al. 1994b). An analysis on natural cordierites is complicated. Winkler (1996) has summarized and discussed the state of affairs and his interpretations can be updated based on our results. For Class I-Type I/II H<sub>2</sub>O the molecule flips or hops (residing in each orientation for a few picoseconds) around [001] about its center of mass down to at least 3 K. Our IR and Raman measurements show that two states of the H<sub>2</sub>O can occur (i.e., Class I Type I and Type II orientations) as defined by the time scales of the IR and Raman experiment. In both the residence time is long enough to see orientations of the molecule in the YZ and ZX crystal planes (Table 2). In the dynamic model there is no real difference between Class I Types I and II H<sub>2</sub>O, although the Type II orientation may have a slightly lower potential energy. Only one type of H<sub>2</sub>O is present (i.e., Class I-Type I/II), which is rotationally disordered. It is not clear at this time how Class I-Type III H<sub>2</sub>O fits into this picture, as we have too little data to make any clear statements. If it is involved in this dynamic process, then disorder within the channel cavity for Class I H<sub>2</sub>O is isotropic

(see Carson et al. 1982) and not simply anisotropic as based on the measurements of pure synthetic Mg-cordierite with only Class I-Type I/II H<sub>2</sub>O (Winkler and Hennion 1994). It should be stated here that the rotational disorder in cordierite is different than that in beryl because of the orthorhombic distortion in the former.

There are no inelastic neutron scattering measurements on Class II H<sub>2</sub>O and, therefore, an understanding of its dynamic behavior is more difficult to ascertain. The Raman results indicate that the H<sub>2</sub>O molecule here can have, as well, two orientations in both the XZ and YZ crystal planes, but with the latter preferred. It is logical to propose that this Class of H<sub>2</sub>O may also be dynamically disordered with the molecule jumping between two different orientations. This proposal must be tested, however, with additional measurements.

With regards to the bonding of H<sub>2</sub>O in cordierite, some investigators have compared it in a thermodynamic sense to H<sub>2</sub>O in water (e.g., Carey and Navrotsky 1992; Newton and Wood 1979), while others have stressed the unbound, anisotropic rotation nature of the molecule at room temperature and lower (e.g., Winkler et al. 1994a). The former consideration implies hydrogen bonding with the cordierite framework, something that is not supported by the spectroscopic and computational data (Langer and Schreyer 1976; Winkler et al. 1994a). Our measurements support the latter interpretation. Class I H<sub>2</sub>O in cordierite and beryl could have weak hydrogen bonding at low temperatures, but it is clearly less strong than that in liquid water or ice. It is also clear that the energetics and bonding of Class I Types I and II H<sub>2</sub>O are different than those governing Class I Type III H<sub>2</sub>O, as demonstrated by the different energies of their  $\nu_3$  modes. The experiments of Johannes and Schreyer (1981) and the calculations of Newton and Wood (1979) and Carey (1995) on the thermodynamic state of H<sub>2</sub>O in synthetic alkali-free H<sub>2</sub>O may not be directly applicable to some natural cordierites, because of the different H<sub>2</sub>O types present. All H<sub>2</sub>O types must be considered in any thermodynamic treatment of H<sub>2</sub>O in natural cordierites. The uncertainty and disagreement in the literature with regard to the more quantitative aspects of the thermodynamics and dynamics of H<sub>2</sub>O in cordierite are a result of the complexity of the problem. The "final word" on this is not yet in.

This investigation also demonstrates that previous analytical determinations of the amount of H<sub>2</sub>O in cordierite must now be rethought. Bulk methods (e.g., DTA, Karl Fischer titration) or even measurements such as those with an ion-probe will not, in many cases, be able to determine the concentrations of the different molecular types. It is necessary to make spectroscopic measurements, preferably at low temperatures and on single crystals, in order to determine them. Previous H<sub>2</sub>O calibrations and determinations need to be rethought. The calibration of Goldman et al. (1977) did not consider the different types of H<sub>2</sub>O present. In addition, the effect of CO<sub>2</sub> and alkali cations on the total weight loss of cordierite through heating was not considered.

A final important point is that the interpretations made here through the combined use of IR and Raman spectroscopy, together with the information provided by inelastic neutron scattering measurements, made at different temperatures, show the

necessity of undertaking different spectroscopic measurements in order to obtain a complete understanding of the dynamic behavior and orientation of H<sub>2</sub>O in cordierite.

## ACKNOWLEDGMENTS

We thank S. Herting (Berlin), Th. Armbruster (Bern), G.R. Rossman (Pasadena), and J.K. Vry (Wellington) for cordierite samples. V. Khomenko kindly "checked" our IR spectra with further measurements. We thank B. Winkler for many helpful discussions. Th. Armbruster read a first draft and offered helpful suggestions for its improvement. This work was supported by a grant from the "Deutsche Forschungsgemeinschaft" (Ge 659/6-1) and from the "Volkswagen-Stiftung" (I/72 951).

## REFERENCES CITED

- Aines, R.D. and Rossman, G.R. (1984) The high temperature behavior of water and carbon dioxide in cordierite and beryl. *American Mineralogist*, 69, 319–327.
- Armbruster, T. (1985) Ar, N<sub>2</sub>, and CO<sub>2</sub> in the structural cavities of cordierite, an optical and X-ray single-crystal study. *Physics and Chemistry of Minerals*, 12, 233–245.
- (1986) Role of Na in the structure of low-cordierite: A single-crystal X-ray study. *American Mineralogist*, 71, 746–757.
- Armbruster, T. and Bloss, F.D. (1982) Orientation and effects of channel H<sub>2</sub>O and CO<sub>2</sub> in cordierite. *American Mineralogist*, 67, 284–291.
- Armbruster, T. and Bürgi, H.B. (1982) Orientation of CO<sub>2</sub> in cavity of cordierite: a single crystal X-ray study at 100 K, 300 K and 500 K. *Fortschr. Miner.*, 60, Beiheft 1, 37–39.
- Carey, J.W. (1995) A thermodynamic formulation of hydrous cordierite. *Contributions to Mineralogy and Petrology*, 119, 155–165.
- Carey, J.W. and Navrotsky, A. (1992) The molar enthalpy of dehydration of cordierite. *American Mineralogist*, 77, 930–936.
- Carson, D.G., Rossman, G.R., and Vaughan, R.W. (1982) Orientation and motion of water molecules in cordierite: a proton nuclear magnetic resonance study. *Physics and Chemistry of Minerals*, 8, 14–19.
- Cohen, J.P., Ross, F.K., and Gibbs G.V. (1977) An X-ray and neutron diffraction study of hydrous low cordierite. *American Mineralogist*, 62, 67–78.
- Farrell, E.F. and Newnham R.E. (1967) Electronic and vibrational absorption spectra in cordierite. *American Mineralogist*, 52, 380–388.
- Fredin, L., Nelander, B., and Ribbegard, G. (1977) Infrared spectrum of the water dimer in solid nitrogen. *Journal of Chemical Physics*, 66, 4065–4072, 4073–4077.
- Geiger, C.A., Armbruster, T., Khomenko, V., and Quartieri, S. (2000) Cordierite I: The coordination of Fe<sup>2+</sup>. *American Mineralogist*, 85, 1255–1264.
- Goldman D.S., Rossman, G.R., and Dollase, W.A. (1977) Channel constituents in cordierite. *American Mineralogist*, 62, 1144–1157.
- Hochella, M.F., Brown, G.E., Ross, F.K., and Gibbs, G.V. (1979) High-temperature crystal chemistry of hydrous Mg- and Fe-cordierites. *American Mineralogist*, 64, 337–351.
- Johannes, W. and Schreyer, W. (1981) Experimental introduction of CO<sub>2</sub> and H<sub>2</sub>O into Mg-Cordierite. *American Journal of Science*, 281, 299–317.
- Kolesov, B.A. and Geiger, C.A. (2000) The orientation and vibrational states of H<sub>2</sub>O in synthetic alkali-free beryl. *Physics and Chemistry of Minerals*, in press.
- Langer, K. and Schreyer, W. (1976) Apparent effects of molecular water on the lattice geometry of cordierite: a discussion. *American Mineralogist*, 61, 1036–1040.
- Le Breton, N. and Schreyer, W. (1993) Experimental CO<sub>2</sub> incorporation into Mg-cordierite: nonlinear behaviour of the system. *European Journal of Mineralogy*, 5, 427–438.
- Murphy, W.F. (1977) The ro-vibrational Raman spectrum of water vapour  $\nu_2$  and  $2\nu_2$ . *Molecular Physics*, 33, 1701–1714.
- (1978) The rovibrational Raman spectrum of water vapour  $\nu_1$  and  $\nu_3$ . *Molecular Physics*, 36, 727–732.
- Nelander, B. (1985) Impurity perturbations of the fundamental band of carbon monoxide in solid nitrogen. *Journal of Physical Chemistry*, 89, 827–830.
- Newton, R.C. and Wood, B.J. (1979) Thermodynamics of water in cordierite and some petrologic consequences of cordierite as a hydrous phase. *Contributions to Mineralogy and Petrology*, 68, 391–404.
- Raeymaekers, P., Figeys, H., and Geerlings, P. (1988) Ab initio calculations of the Raman intensities of fundamental vibrations of polyatomic molecules using the improved virtual orbital technique. *Journal of Molecular Structure (Theoretical Chemistry)*, 169, 509–530.
- Redington, R.A. and Milligan, D.E. (1962) Infrared spectroscopic evidence for the rotation of the water molecule in solid argon. *Journal of Chemical Physics*, 37, 2162–2166.
- Shannon, R.D., Marinao, A.N., and Rossman, G.R. (1992) Effect of H<sub>2</sub>O and CO<sub>2</sub> on dielectric properties of single-crystal cordierite and comparison with polycrystalline cordierite. *Journal of the American Ceramic Society*, 75, 2395–2399.
- Sugiura, K. (1959) The water problem of cordierite. *Bulletin of the Tokyo Institute*

- of Technology, Series-B, no. 1, 1–26.
- Tso, T.-L. and Lee, E.K.C. (1985) Role of hydrogen bonding studied by the FTIR spectroscopy of the matrix-isolated molecular complexes, dimer of H<sub>2</sub>O, H<sub>2</sub>O·CO<sub>2</sub>, H<sub>2</sub>O·CO, and H<sub>2</sub>O·nCO in solid O<sub>2</sub> at 12–17 K. *Journal of Physical Chemistry*, 89, 1612–1618.
- Vry, J.K., Brown, P.E., and Valley, J.W. (1990) Cordierite volatile content and the role of CO<sub>2</sub> in high-grade metamorphism. *American Mineralogist*, 75, 71–88.
- Winkler, B. (1996) The dynamics of H<sub>2</sub>O in minerals. *Physics and Chemistry of Minerals*, 23, 310–318.
- Winkler, B. and Hennion, B. (1994) Low temperature dynamics of molecular H<sub>2</sub>O in bassanite, gypsum and cordierite investigated by high resolution incoherent inelastic neutron scattering. *Physics and Chemistry of Minerals*, 21, 539–545.
- Winkler, B., Milman V., and Payne, M.C. (1994a) Orientation, location, and total energy of hydration of channel H<sub>2</sub>O in cordierite investigated by ab-initio total energy calculations. *American Mineralogist*, 79, 200–204.
- Winkler, B., Coddens, G., and Hennion, B. (1994b) Movement of channel H<sub>2</sub>O in cordierite observed with quasi-elastic neutron scattering. *American Mineralogist*, 79, 801–808.
- Wood, D.L. and Nassau, K. (1967) Infrared spectra of foreign molecules in beryl. *Journal of Chemical Physics*, 47, 2220–2228.
- (1968) The characterization of beryl and emerald by visible and infrared absorption spectroscopy. *American Mineralogist*, 53, 777–800.
- Zilles, B. and Person, W.B. (1983) Interpretation of infrared intensity changes on molecular complex formation. I. Water dimer. *Journal of Chemical Physics*, 79, 65–77.

MANUSCRIPT RECEIVED JUNE 28, 1999

MANUSCRIPT ACCEPTED MAY 9, 2000

PAPER HANDLED BY ANASTASIA CHOPELAS